Methods S1. Quantifying the relative contribution of differences in vapor pressure to differences in atmospheric VPD in nature

If vapor pressure deficit (VPD) differs between two times on the same day in a given location, this can result either from a difference in vapor pressure (p_{air}), a difference in saturation vapor pressure (p_{sat}) caused by a difference in temperature, or some combination of the two. For a given comparison between two time points, the fractional contribution of the difference in p_{air} (δp_{air}) to the difference in VPD (δVPD) equals minus the ratio of the difference in p_{air} to the difference in VPD:

$$\delta\mathrm{VPD} = \delta p_{sat} - \delta p_{air} \;\rightarrow\; \begin{matrix}\text{fractional}\\ \text{contribution}\\ \text{of } \delta p_{air}\end{matrix} = \frac{-\delta p_{air}}{\delta\mathrm{VPD}}. \quad \text{(S1)}$$

Thus, for example, suppose VPD were higher at one time (t_1) than another (t_2); then if $-\delta p_{air}/\delta\mathrm{VPD} = 0.25$, one-quarter of the difference in VPD (δVPD = VPD(t_1) – VPD(t_2)) could be attributed to the difference in vapor pressure. If $-\delta p_{air}/\delta\mathrm{VPD} = 0$, the entire difference in VPD would be attributable to temperature; and so forth.

To quantify the frequency distribution of the fractional contribution of δp_{air} to diurnal variation in VPD, we downloaded all hourly meteorological measurements for each of the 145 CIMIS stations (California Irrigation Management System; www.cimis.water.ca.gov) that were active in 2022. We then calculated the quantity $-\delta p_{air}/\delta\mathrm{VPD}$ for every possible pairwise comparison between daytime time points in a given day at each site (defining 'daytime' as times at which the radiation reported by CIMIS was positive). This resulted in a total of 4,251,643 pairwise comparisons (approximately equivalent to an average of $n\cdot(n-1)/2 = 13\cdot12/2$ hourly daytime comparisons per day per site, times 365 days, times 145 sites).

Figure S2 presents the cumulative distribution of the results, expressed in relation to the value of $-\delta p_{air}/\delta\mathrm{VPD}$. In 20% of comparisons, a change in atmospheric humidity contributed more than 50% of the corresponding change in VPD; in 36% of cases, p_{air} contributed at least 25% of the corresponding change in VPD.

Methods S2. Issues with the Peak-Mott model

Peak & Mott (Peak & Mott 2011; PM) posited that guard cell water potential is decoupled from leaf water status, and instead equilibrates with air in the stomatal pore channel; since the relative humidity of the air in the pore channel should increase with temperature if Δw is constant, warming should hydrate guard cells, opening stomata as the leaf warms. Thus, the PM model predicts a DRST. However, several of PM's predictions and assumptions contradict other evidence, and the model also contains internal contradictions:

(1) The pore-air-equilibrium hypothesis is difficult to reconcile with experiments in which vapor pressure and vapor flux were independently manipulated by modulating the diffusion coefficient for water vapor (by replacing the N_2 in air with He, making "helox"); those experiments showed that stomata sense the rate of water loss, not humidity per se (Mott & Parkhurst 1991). PM reconciled their model with the helox data by positing that increasing transpiration rate cools the mesophyll relative to the guard cells (in which case switching from nitox to helox would reduce vapor pressure in the pore channel, but not temperature, thus reducing relative humidity and water potential and dehydrating guard cells, closing stomata). However, detailed 2D and 3D simulations of heat and vapor transport in the leaf (Rockwell, Holbrook & Stroock 2014; Buckley, John, Scoffoni & Sack 2017) suggest transpiration cools the epidermis and guard cells relative to the mesophyll, rather than the reverse as PM assumed. This would both reverse the direction of the predicted DRST and leave the model in contradiction with the helox results.

(2) Stomata close when plant hydraulic conductance or soil water potential are decreased (Saliendra, Sperry & Comstock 1995; Comstock & Mencuccini 1998), whereas PM predicts stomatal opening. This could be reconciled by augmenting the model with a metabolically-mediated 'hydroactive' response to leaf water status (Xie *et al.* 2006; McAdam & Brodribb 2016; Sussmilch, Brodribb & McAdam 2017), but the resulting model would predict much stronger stomatal responses to humidity than to water supply, which is not consistent with observations (Buckley, Sack & Gilbert 2011). On the contrary, models based on a response mediated by leaf water status, rather than by humidity per se, accurately predict a pervasive symmetry in short-term steady state stomatal responses to any factor that influences leaf water status (Mott, Denne & Powell 1997; Buckley & Mott 2002; Buckley, Mott & Farquhar 2003; Buckley 2005, 2019).

(3) The PM model assumes the mesophyll has the same water potential as the epidermis, but lower temperature; this implies vapor pressure is lower in the mesophyll, which in turn predicts vapor should diffuse into the leaf rather than out. The assumption of equal water potentials in the epidermis and mesophyll also contradicts data of Mott (2007) and Shackel & Brinkmann (1985) suggesting the epidermis is separated from the bulk leaf by a substantial hydraulic resistance. Those data are further supported by intensive biophysical modeling of water transport in the leaf (Rockwell *et al.* 2014; Buckley *et al.* 2017).

(4) Stomatal responses to cues other than ambient humidity and temperature (for example, a shift from light to darkness) can occur far more rapidly than would be possible if the permeability for exchange of water between guard cells and the adjacent epidermis were as low as required for the PM mechanism.

This implies that the permeability between guard and epidermal cells is actually quite high during such responses. It is of course possible that permeability could be increased only transiently during those responses, in order to facilitate volume changes, and then subsequently decreased; but that would result in guard cells being hydraulically equilibrated not with the pore air, but with water in apoplast connecting them to adjacent epidermal cells, immediately after the response. The PM mechanism implies that guard cells would then slowly re-equilibrate with the pore air; given the much lower water potential purported by PM to exist in the pore air, as compared to the water potential of adjacent epidermal cells, such re-equilibration would cause a dramatic decline in stomatal volume and aperture over a slow re-equilibration period. Such patterns are not generally observed, to our knowledge.

Methods S3. Derivation of an expression for the contribution of the DRST to changes in transpiration rate in the environment, under well-coupled conditions

Provided the leaf and air are well-coupled, i.e., boundary layer conductance is large and leaf temperature is therefore close to air temperature, so that transpiration rate is given by $E = g_s \Delta w$ (we will relax this assumption later, in Methods S4), the response of E to temperature is then

$$\frac{dE}{dT} = \left(\frac{\partial E}{\partial \Delta w}\right)_{gs} \frac{d\Delta w}{dT} + \left(\frac{\partial E}{\partial g_s}\right)_{\Delta w} \left[\left(\frac{\partial g_s}{\partial \Delta w}\right)_T \frac{d\Delta w}{dT} + \left(\frac{\partial g_s}{\partial T}\right)_{\Delta w}\right], \text{and} \quad \text{(S2)}$$

$$\frac{dE}{dT} = g_s \frac{d\Delta w}{dT} + \Delta w \frac{d\Delta w}{dT}\left(\frac{\partial g_s}{\partial \Delta w}\right)_T + \Delta w \left(\frac{\partial g_s}{\partial T}\right)_{\Delta w}. \quad \text{(S3)}$$

Thus, the sensitivity of E to T has three components: (i) the direct effect of any change in Δw with temperature, independent of any stomatal response, (ii) the effect of the stomatal response to any change in Δw, and (iii) the effect of the stomatal response to temperature *per se* (the DRST). Similarly, the response of E to Δw is

$$\frac{dE}{d\Delta w} = \left(\frac{\partial E}{\partial \Delta w}\right)_{gs} + \left(\frac{\partial E}{\partial g_s}\right)_{\Delta w} \left[\left(\frac{\partial g_s}{\partial \Delta w}\right)_T + \left(\frac{\partial g_s}{\partial T}\right)_{\Delta w} \frac{dT}{d\Delta w}\right], \text{and} \quad \text{(S4)}$$

$$\frac{dE}{d\Delta w} = g_s + \Delta w \left(\frac{\partial g_s}{\partial \Delta w}\right)_T + \Delta w \frac{dT}{d\Delta w}\left(\frac{\partial g_s}{\partial T}\right)_{\Delta w}. \quad \text{(S5)}$$

The sensitivity of E to Δw therefore also has the same three components: (i) the direct effect of Δw, (ii) the effect of the stomatal response to Δw, and (iii) the effect of the DRST. Moreover, minor rearrangement of Eqns S3 and S5 reveals that the three components have the same relationships to one another in the responses of E to both Δw and T:

$$\frac{dE}{d\Delta w} = g_s \left[1 + \Delta w \left(\frac{\partial \ln g_s}{\partial \Delta w}\right)_T + \Delta w \frac{dT}{d\Delta w}\left(\frac{\partial \ln g_s}{\partial T}\right)_{\Delta w}\right], \text{and} \quad \text{(S6)}$$

$$\frac{dE}{dT} = g_s \frac{d\Delta w}{dT}\left[1 + \Delta w \left(\frac{\partial \ln g_s}{\partial \Delta w}\right)_T + \Delta w \frac{dT}{d\Delta w}\left(\frac{\partial \ln g_s}{\partial T}\right)_{\Delta w}\right]. \quad \text{(S7)}$$

The ***fractional contribution of the DRST*** to changes in transpiration caused by changes in either Δw or T can be expressed by dividing the third quantity in square brackets in S6 or S7 by the sum of all three of the quantities in square brackets, giving

$$\frac{\text{fractional contribution}}{\text{of DRST to changes in } E} = \frac{\Delta w \frac{dT}{d\Delta w}\left(\frac{\partial \ln g_s}{\partial T}\right)_{\Delta w}}{1 + \Delta w \left(\frac{\partial \ln g_s}{\partial \Delta w}\right)_T + \Delta w \frac{dT}{d\Delta w}\left(\frac{\partial \ln g_s}{\partial T}\right)_{\Delta w}}. \quad \text{(S8)}$$

Applying Eqn S8 requires estimates for the relative sensitivities of g_s to Δw and T ($\partial \ln g_s/\partial \Delta w$ and $\partial \ln g_s/\partial T$) and the environmental correlation between Δw and T ($d\Delta w/dT$). We constrained these quantities as follows.

First, to constrain $\partial \ln g_s/\partial T$, we noted that the meager available data (Fig 2 in the main text) suggest $\partial \ln g_s/\partial T$ is often in the range of 0.01 K^{-1} to 0.03 K^{-1}; we thus used these two values to represent "weak" and "strong" DRSTs.

Second, to constrain $\partial \ln g_s/\partial \Delta w$, we used the finding of Oren *et al*. (1999) that the following empirical model for stomatal conductance in relation to Δw accurately described observations for a large number of species and locations:

$$g_s = g_r\left(1 - m \ln\left[\frac{\Delta w}{\Delta_o}\right]\right) \qquad \text{(S9)}$$

where Δ_o is a reference value of Δw (0.01 mol mol^{-1}), g_r is the value of g_s at that reference, and m is a dimensionless parameter. The total sensitivity of g_s to Δw in this model is

$$\frac{d \ln g_s}{d\Delta w} = -\frac{m}{\Delta w\left(1 - m \ln\left[\frac{\Delta w}{\Delta_o}\right]\right)} \qquad \text{(S10)}$$

Note that the data used by Oren *et al*. were based on field measurements of Δw, in which T likely also varied naturally in the environment. Thus, the derivative in Eqn S10 includes both the response to Δw *per se* and the response to any underlying variations in T:

$$\frac{d \ln g_s}{d\Delta w} = \left(\frac{\partial \ln g_s}{\partial \Delta w}\right)_T + \left(\frac{\partial \ln g_s}{\partial T}\right)_{\Delta w}\frac{dT}{d\Delta w} \qquad \text{(S11)}$$

Note further that this quantity also appears in the denominator in Eqn S8 (to see this, pull Δw out of the latter two terms in the denominator of Eqn S8), giving the latter as

$$\frac{\text{fractional contribution}}{\text{of DRST to changes in } E} = \frac{\Delta w \frac{dT}{d\Delta w}\left(\frac{\partial \ln g_s}{\partial T}\right)_{\Delta w}}{1 + \Delta w \frac{d \ln g_s}{d\Delta w}} \qquad \text{(S12)}$$

Finally, replacing $d \ln g_s/d\Delta w$ with the Oren result (Eqn S10) and rearranging gives

$$\text{fractional contribution of DRST to changes in } E = \frac{\left(\frac{\partial \ln g_s}{\partial T}\right)_{\Delta w}}{\frac{1}{\Delta w}\frac{d\Delta w}{dT}\left(1 - \frac{m}{1 - m\ln\left[\frac{\Delta w}{\Delta_o}\right]}\right)} \quad \text{(S13)}$$

To constrain the parameter m, we used the 10th and 90th percentile of values reported by Oren *et al*. across a range of species, namely m = 0.442 and m = 0.751 (dimensionless), to represent "weak" and "strong" Δw responses, respectively.

Third, we constrained the quantity $(1/\Delta w)\cdot d\Delta w/dT$ using the CIMIS meteorological data described in Methods S1. It is important to note that, in this context, $d\Delta w/dT$ does <u>not</u> represent how Δw changes if T is altered experimentally in a laboratory; instead, it represents how, empirically, Δw and T actually covary in the environment, where both T and ambient vapor pressure can, in principle, vary independently of one another. We obtained the density distribution for $(1/\Delta w)\cdot d\Delta w/dT$ in the same way as described for the distribution of $\delta p_{air}/\delta$VPD in Methods S1. For every possible pairwise comparison between daytime time points in a given day at a given CIMIS station, we calculated the difference in Δw ($\delta[\Delta w]$), the difference in T (δT), and the mean value of Δw between the two time points ($\overline{\Delta w}$), and combined them to produce a finite-difference estimate of $(1/\Delta w)\cdot d\Delta w/dT$ as $(1/\overline{\Delta w})\cdot\delta[\Delta w]/\delta T$. Repeating this for all pairwise comparisons between timepoints resulted in a total of 4,251,643 comparisons (roughly equivalent to an average of $n\cdot(n-1)/2 = 13\cdot12/2$ hourly daytime comparisons per day per site, times 365 days, times 145 sites). Finally, we applied the distribution of the resulting values, together with the estimates for $\partial\ln g_s/\partial T$ and m described above, to Eqn S13 to obtain distributions for the fractional contribution of the DRST to changes in transpiration, for four scenarios (weak vs strong DRST $\times$ weak vs strong Δw response). The results are shown in Figure 6 in the main text.

Methods S4. Analysis of the role of the DRST in regulating leaf temperature

To quantify how the DRST influences leaf temperature, we simulated leaf temperature using the following model, which arises from using first-order Taylor series to approximate the terms in leaf energy balance that are nonlinear in leaf temperature (namely, the outgoing longwave radiation and the leaf to air water vapor mole fraction gradient):

$$T_L = T_A + \frac{Q - (\epsilon_L - \epsilon_A)\sigma T_A^4 - \lambda g_{tw} \Delta w_{atm}}{4\epsilon_L \sigma T_A^3 + c g_{bh} + \lambda g_{tw} s}, \quad \text{(S14)}$$

where Q is absorbed shortwave radiation, ε_L and ε_A are leaf and atmospheric longwave emissivity, respectively, σ is the Stefan-Boltzmann constant, T_A is air temperature in kelvins, λ is the latent heat of vaporization, g_{tw} is total leaf conductance to water vapor (the parallel sum of stomatal [g_s] and boundary layer [g_{bw}] conductances), Δw_{atm} is the atmospheric vapor pressure deficit as a mole fraction (not the leaf to air Δw), c is the heat capacity of air, g_{bh} is the leaf boundary layer conductance to heat (= g_{bw}/1.08), and s is the derivative of saturated water vapor mole fraction with respect to temperature. This model assumes negligible net longwave radiation transfer occurs at the lower surface (i.e., the leaf in question is located above many other leaves with similar temperature), the upper surface is fully exposed to the atmosphere, and the leaf is amphistomatous, with equal g_s at each surface.

We simulated g_s using an empirical model, modified from the model used by Oren *et al*. (1999) to include a hyperbolic, saturating response to light (represented by shortwave radiation, Q) and a linear direct response to temperature:

$$g_s = g_{rmax}\left(\frac{Q}{Q + k_Q}\right)\left(1 - m \ln\frac{\Delta w}{\Delta_o}\right)\left(1 + b(T - T_o)\right), \quad \text{(S15)}$$

where g_{rmax}, k_Q and b are adjustable parameters, respectively representing the light-saturated value of g_s at $\Delta w = \Delta_o$ and T =25°C, the value of Q at which the effect of light on g_s is half saturated, and the relative sensitivity of the DRST ($\partial \ln g_s / \partial T$) at a reference temperature, T_o. We constrained b using the same scenarios as in Methods S3, namely "weak" and "strong" DRSTs of b = 0.01 and 0.03 K^{-1} respectively. We constrained the Δw sensitivity parameter m using the all-species average given by Oren *et al*. (1999) of m = 0.6 (unitless). We constrained g_{rmax} and k_Q arbitrarily, using values of g_{rmax} = 0.1 mol m^{-2} s^{-1} and k_Q = 60 J m^{-2} s^{-1} to represent a "shade leaf" with low maximum conductance, and g_{rmax} = 0.5 mol m^{-2} s^{-1} and k_Q = 300 J m^{-2} s^{-1} to represent a "sun leaf" with high maximum conductance, respectively. Finally, we chose two values for g_{bw} to represent relatively decoupled conditions (g_{bw} = 0.5 mol m^{-2} s^{-1}) or moderately coupled conditions (g_{bw} = 3 mol m^{-2} s^{-1}). Thus, we had eight scenarios in total ({weak vs strong DRST} x {low vs high maximum g_s} x {low vs high g_{bw}}).

We applied Eqns S14 and S15 to the CIMIS meteorological data described in Methods S3. Because g_s affects leaf temperature, which in turn affects g_s, this model requires iterative solution; we used three iterations for each time point in the meteorological dataset, using atmospheric values of Δw and T in the

first iteration, and resulting leaf values in the subsequent iterations. Several other parameters and constraints are also needed to apply Eqn S14 for leaf energy balance. We assumed leaf emissivity ε_L = 0.97 and air heat capacitance c = 29.2 J mol^{-1} K^{-1}. We calculated air emissivity as $\varepsilon_A = 0.642(p_A/T_A)^{1/7}$, where p_A is ambient vapor pressure in pascals and T_A is in kelvins (Brutsaert 1975). We assumed a leaf absorptance to shortwave radiation of 0.5·(0.9 + 0.2) = 0.55, which is equivalent to assuming absorptances of 0.9 and 0.2 for visible and near-infrared radiation, respectively, and assuming half of total shortwave radiation is in the visible band (Gates, Keegan, Schleter & Weidner 1965; de Pury & Farquhar 1997).

To isolate the effect of the DRST, we repeated all simulations with the DRST sensitivity (b) set to zero, representing a theoretical leaf with no DRST. To ensure the resulting simulations were as closely comparable as possible, we set the reference temperature for the DRST (T_o in Eqn S15) to the median value of air temperature in the meteorological dataset (18.8°C); thus, for half of the time points, the DRST should increase g_s, and for the other half it should decrease g_s, as compared to the simulated leaf with no DRST. Results are presented in the main text as the difference in leaf temperature between simulations with and without the DRST.

Methods S5. Proof that a positive DRST increases the temperature optimum of photosynthesis

The FvCB model for photosynthesis (Farquhar, von Caemmerer & Berry 1980) can be written as

$$A = \frac{w(c_i - \Gamma_*)}{c_i + M} - R, \quad \text{(S16)}$$

where w is either carboxylation capacity or one-fourth of the potential electron transport rate, M is either $2\Gamma_*$ or the effective Michaelis constant for carboxylation, and R is non-photorespiratory CO_2 release. The sensitivity of A to temperature is thus

$$\frac{dA}{dT} = \frac{\partial A}{\partial w}\frac{dw}{dT} + \frac{\partial A}{\partial \Gamma_*}\frac{d\Gamma_*}{dT} + \frac{\partial A}{\partial M}\frac{dM}{dT} - \frac{dR}{dT} + \frac{\partial A}{\partial c_i}\frac{dc_i}{dT}. \quad \text{(S17)}$$

The change in c_i with temperature is also affected by the diffusional constraint ($A = g(c_a - c_i)$), where g is total conductance to CO_2, so

$$\frac{dA}{dT} = (c_a - c_i)\frac{dg}{dT} - g\frac{dc_i}{dT}. \quad \text{(S18)}$$

Setting S17 and S18 equal, solving for dc_i/dT, applying the result to S17 and rearranging gives

$$\frac{dA}{dT} = \frac{(c_a - c_i)\frac{dg}{dT} - Y}{k + g}, \quad \text{(S19)}$$

where $k \equiv \partial A/\partial c_i$ (the slope of the "A vs c_i curve"), and

$$Y \equiv \frac{\partial A}{\partial w}\frac{dw}{dT} + \frac{\partial A}{\partial \Gamma_*}\frac{d\Gamma_*}{dT} + \frac{\partial A}{\partial M}\frac{dM}{dT} - \frac{dR}{dT}. \quad \text{(S20)}$$

The sensitivity of g to T is

$$\frac{dg}{dT} = \left(\frac{\partial g}{\partial T}\right)_{\Delta w} + \left(\frac{\partial g}{\partial \Delta w}\right)_T \frac{d\Delta w}{dT}. \quad \text{(S21)}$$

Applying S21 to S19 and grouping terms gives

$$\frac{dA}{dT} = \frac{c_a - c_i}{k + g}\left(\frac{\partial g}{\partial T}\right)_{\Delta w} + \left[\frac{(c_a - c_i)\left(\frac{\partial g}{\partial \Delta w}\right)_T \frac{d\Delta w}{dT} - Y}{k + g}\right]. \quad \text{(S22)}$$

In the absence of a DRST, $(\partial g/\partial T)_{\Delta w} = 0$, giving

$$\left.\frac{dA}{dT}\right|_{\text{no DRST}} = \frac{(c_a - c_i)\left(\frac{\partial g}{\partial \Delta w}\right)_T \frac{d\Delta w}{dT} - Y}{k + g}. \quad \text{(S23)}$$

At the temperature that would maximize photosynthesis *in the absence of a DRST*, $T = T_{OPT(\text{no DRST})}$, the quantity on the right-hand side of Eqn S23 is zero (because $dA/dT = 0$ by definition at the temperature that maximizes photosynthesis). Therefore, in the presence of a DRST, the value of dA/dT at $T = T_{OPT(\text{no DRST})}$ is given by

$$\left.\frac{dA}{dT}\right|_{\text{DRST}} \left(\text{at } T = T_{OPT(no\ DRST)}\right) = \frac{c_a - c_i}{k + g}\left(\frac{\partial g}{\partial T}\right)_{\Delta w}. \quad \text{(S24)}$$

If there is in fact a positive DRST ($(\partial g/\partial T)_{\Delta w} > 0$), then dA/dT is positive at $T = T_{OPT(\text{no DRST})}$ (provided $A > 0$; because then $c_a - c_i$ and $k + g$ are positive). This means that A will continue increasing until some higher temperature, and therefore the leaf is below its true temperature optimum (T_{OPT}) when $T = T_{OPT(\text{no DRST})}$. Therefore, the temperature optimum in the presence of a positive DRST is greater than that in the absence of a DRST (i.e., $T_{OPT} > T_{OPT(\text{no DRST})}$), i.e., a positive DRST increases the temperature optimum for photosynthesis.

Methods S6. Rederivation of least-cost optimization

The least-cost optimality model predicts that

$$\frac{\partial}{\partial \chi}\left[a\frac{E}{A}+b\frac{V_m}{A}\right]=0, \qquad \text{(S25)}$$

where χ is the ratio c_i/c_a and a and b are empirical parameters. Prentice et al (2014) derived their solution by assuming that $A >> R$ (dark respiration rate), and using only a carboxylation-limited expression for A. Here we relax both conditions to obtain a general expression that can be used to explore this model's predictions regarding the DRST. Under carboxylation-limited conditions,

$$\frac{V_m}{A}=\frac{1}{\frac{\chi c_a-\Gamma_*}{\chi c_a+K'}-\frac{R}{V_m}}=\frac{\chi c_a+K'}{\chi c_a\left(1-\frac{R}{V_m}\right)-\left(\Gamma_*+\frac{R}{V_m}K'\right)}. \qquad \text{(S26)}$$

The partial derivative of this ratio with respect to χ is

$$\frac{\partial}{\partial \chi}\left[\frac{V_m}{A}\right]=-\frac{c_a(K'+\Gamma_*)}{\left(\chi c_a\left(1-\frac{R}{V}\right)-\left(\Gamma_*+\frac{R}{V_m}K'\right)\right)^2}. \qquad \text{(S27)}$$

Prentice showed that

$$\frac{\partial}{\partial \chi}\left[\frac{E}{A}\right]=\frac{1.6D}{c_a(1-\chi)^2}. \qquad \text{(S28)}$$

Applying S27 and S28 to S25 and rearranging gives

$$\chi=\frac{\frac{\xi_v}{\sqrt{D}}+\frac{\Gamma_*}{c_a}+\frac{R}{V}\frac{K'}{c_a}}{\frac{\xi_v}{\sqrt{D}}+1-\frac{R}{V}}, \ \ where \ \ \xi_v\equiv\sqrt{\frac{\beta(K'+\Gamma_*)}{1.6}}, \qquad \text{(S29)}$$

where $\beta \equiv b/a$, and ξ_v is equivalent to ξ in Prentice et al (2014). Setting $R = 0$ and rearranging retrieves their original solution. Under regeneration-limited conditions, a different expression for A must be used:

$$\frac{V_m}{A}=\frac{1}{\left(\frac{J}{4V_m}\right)\frac{\chi c_a-\Gamma_*}{\chi c_a+2\Gamma_*}-\frac{R}{V_m}}=\frac{\chi c_a+2\Gamma_*}{\chi c_a\left(\frac{J}{4V_m}-\frac{R}{V_m}\right)-\left(\frac{J}{4V_m}+2\frac{R}{V_m}\right)\Gamma_*}. \qquad \text{(S30)}$$

The resulting derivative with respect to χ is

$$\frac{\partial}{\partial\chi}\left[\frac{V_m}{A}\right]=\frac{-c_a\Gamma_*\frac{3J}{4V_m}}{\left[\chi c_a\left(\frac{J}{4V_m}-\frac{R}{V_m}\right)-\left(\frac{J}{4V_m}+2\frac{R}{V_m}\right)\Gamma_*\right]^2}, \quad \text{(S31)}$$

and applying S31 and S28 to S25 and rearranging gives

$$\chi=\frac{\frac{\xi_j}{\sqrt{D}}+\left(\frac{J}{4V_m}+2\frac{R}{V_m}\right)\frac{\Gamma_*}{c_a}}{\frac{\xi_j}{\sqrt{D}}+\frac{J}{4V_m}-\frac{R}{V_m}}, \ \ where \ \ \xi_j\equiv\sqrt{\frac{\beta}{1.6}\cdot\frac{3J\Gamma_*}{4V_m}}. \quad \text{(S32)}$$

We applied S29 and S32 across a range of temperatures, for two values of irradiance and VPD. To determine which expression to apply in any given condition, we computed the assimilation rate implied by both values of χ and chose the lesser value. We used expressions given by Bernacchi et al. (2001; 2003) for temperature dependencies of photosynthetic parameters, and for the relationship of *J* to irradiance and underlying parameters.

Figure S1. Effect of temperature on the binary molecular diffusivity of water vapor in air (dashed line) and on stomatal conductance for constant stomatal aperture (solid line). The dashed line is a response to absolute temperature raised to the power of 1.81; the solid line is the same but with a power of 0.81 (1.81 – 1), representing the fact that stomatal conductance for a given stomatal aperture scales with the ratio of the diffusivity to absolute temperature.

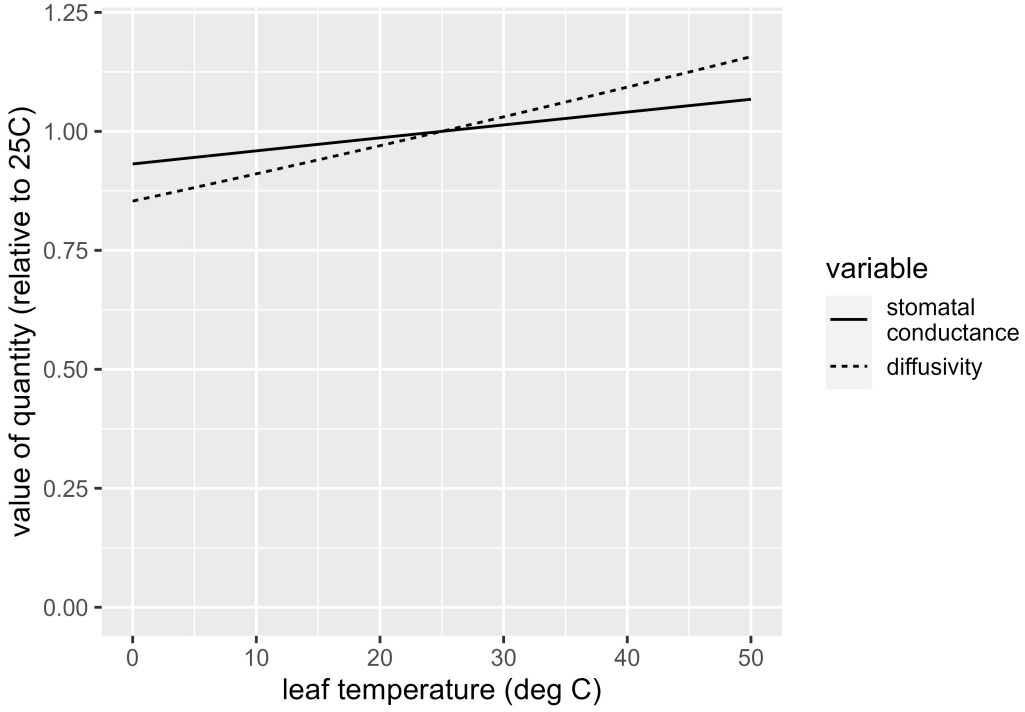

Figure S2. Cumulative distribution of proportional contributions of decreases in atmospheric vapor pressure, p_{air}, to given increases in atmospheric vapor pressure deficit, VPD ($-\delta p_{air}/\delta VPD$), computed for every possible pairwise comparison between two hourly daytime time points in a given day in calendar year 2022, at a given site, and aggregated across all days for all 145 CIMIS sites (California Irrigation Management System; www.cimis.ca.gov) that were active in 2022. Spring, summer and fall are defined here as julian day $\in$ [80, 171], [172, 263] and [264, 354], respectively, and winter is Julian day <= 80 or >= 355. The apparent discontinuity at zero is an artifact of the coarse resolution at which vapor pressure and temperature are reported in CIMIS data.

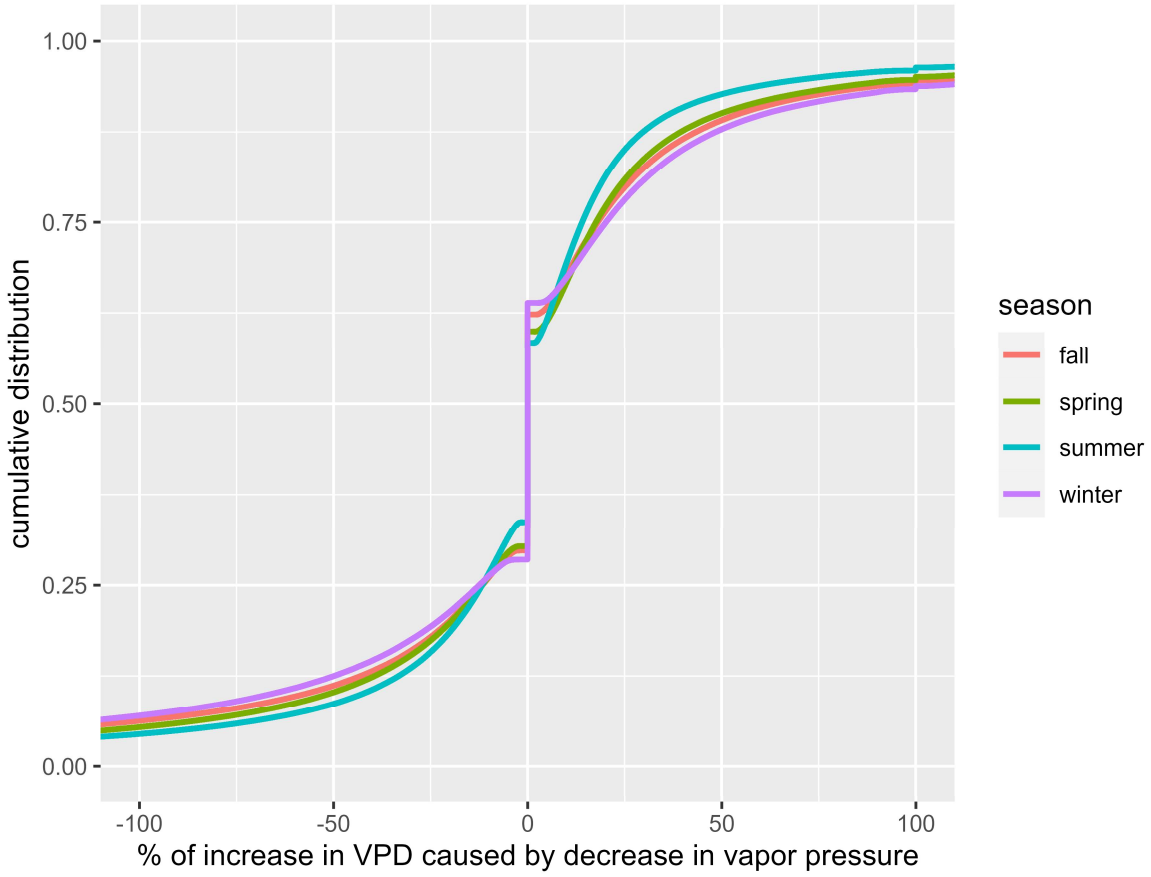

Fig S3. Effect of temperature on vapor-phase transport conductances in the leaf. "Isothermal" refers to the vapor flux per unit of water potential gradient, for vapor transport that occurs independent of any temperature gradient within the leaf along the diffusion path; "anisothermal" refers to the vapor flux per unit of temperature gradient, for vapor transport driven by a temperature gradient. Calculations were based on expressions given by Buckley et al. (2017).

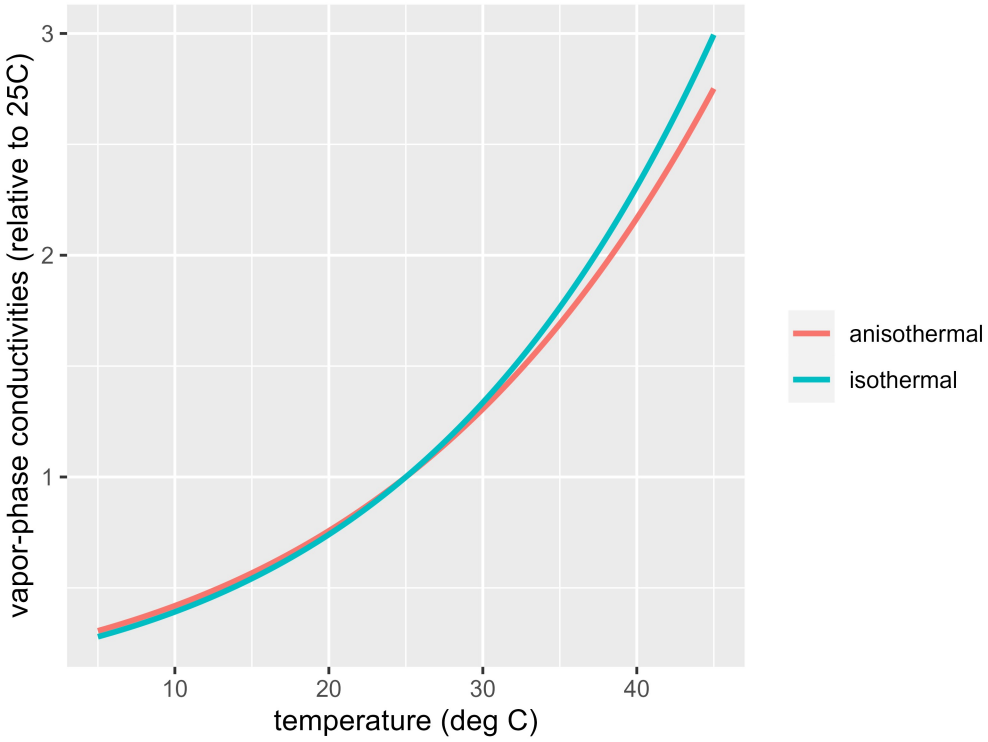

Fig S4. Effect of temperature on photosynthetic parameters that determine [ATP] in the models of Farquhar & Wong (1984) and Buckley, Mott & Farquhar (2003). [ATP] is an increasing function of the ratio W_j/W_c, which is shown with a dashed black line; W_c and W_j are the carboxylation rates when light or Rubisco, respectively, are limiting, and are given by $W_c = V_{cmax} \cdot c_i/(c_i + K')$ and $W_j = 0.25J \cdot c_i/(c_i + 2\Gamma_*)$, where K' and Γ_* are the effective Michaelis constant for carboxylation, and the photorespiratory CO_2 compensation point, respectively. Thus $W_j/W_c = (4J/V_{cmax}) \cdot [(c_i + K')/(c_i + 2\Gamma_*)]$. "ci_fn" is $(c_i + K')/(c_i + 2\Gamma_*)$.

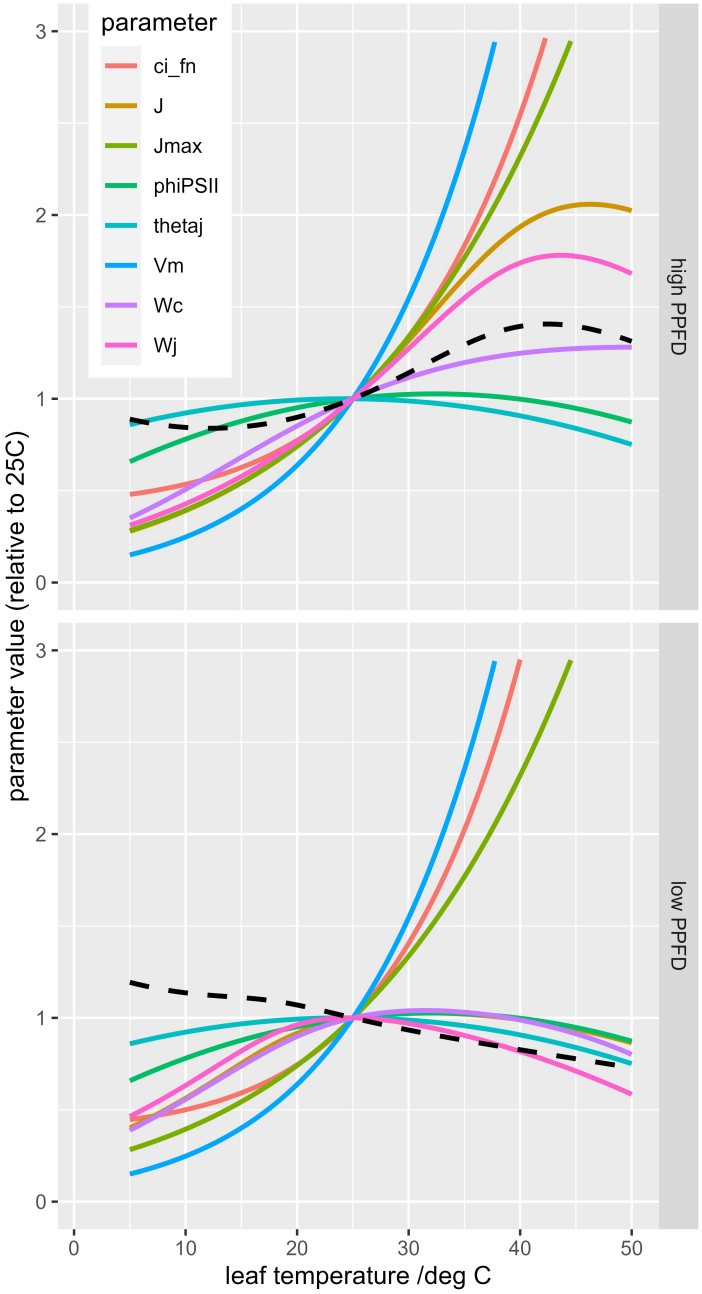

Fig S5. Dependence of predicted responses of stomatal conductance to VPD on the contribution of vapor pressure, rather than temperature, to the shift in VPD, for three empirical models (Ball-Berry (BB, Ball, Woodrow & Berry 1987), Ball-Berry-Leuning (BBL, Leuning 1995) and Unified Stomatal Optimization (USO, Medlyn *et al.* 2011)) and Unified Stomatal Optimization (USO; Medlyn et al 2011), two initial relative humidities (RH) and temperatures, and two days (23 July and 24 May 2023) at the Tonzi Ranch Ameriflux site in central California.

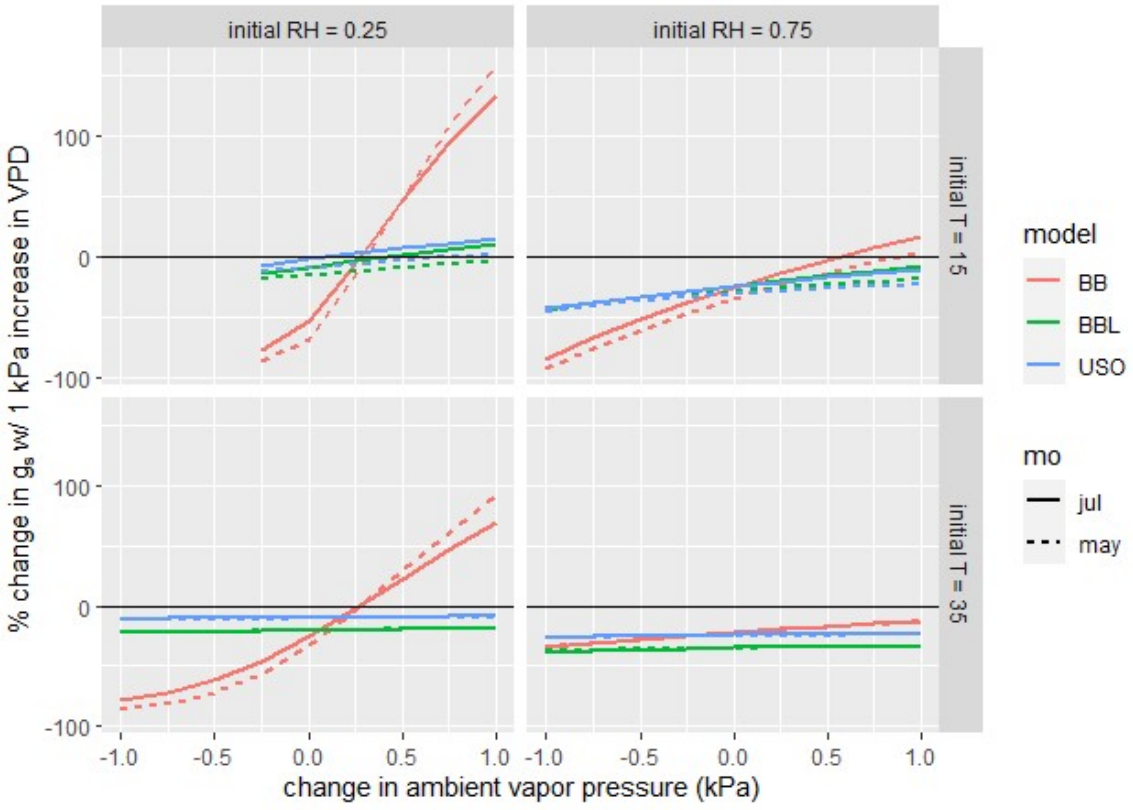

References

Ball J.T., Woodrow I.E. & Berry J.A. (1987) A model predicting stomatal conductance and its contribution to the control of photosynthesis under different environmental conditions. In *Progress in Photosynthesis Research*. (ed J. Biggens), pp. 221–224. Martinus Nijhoff Publishers, The Netherlands.

Bernacchi C., Pimentel C. & Long S.P. (2003) In vivo temperature response functions of parameters required to model RuBP-limited photosynthesis. *Plant, Cell & Environment* **26**, 1419–1430.

Bernacchi C.J., Singsaas E.L., Pimentel C., Portis A.R.J. & Long S.P. (2001) Improved temperature response functions for models of Rubisco-limited photosynthesis. *Plant, Cell and Environment* **24**, 253–259.

Brutsaert W. (1975) On a derivable formula for long-wave radiation from clear skies. *Water resources research* **11**, 742–744.

Buckley T.N. (2005) The control of stomata by water balance (Tansley Review). *New Phytologist* **168**, 275–292.

Buckley T.N. (2019) How do stomata respond to water status? *New Phytologist* **224**, 21–36.

Buckley T.N., John G.P., Scoffoni C. & Sack L. (2017) The sites of evaporation within leaves. *Plant Physiology* **173**, 1763–1782.

Buckley T.N. & Mott K.A. (2002) Stomatal water relations and the control of hydraulic supply and demand. *Progress in Botany* **63**, 309–325.

Buckley T.N., Mott K.A. & Farquhar G.D. (2003) A hydromechanical and biochemical model of stomatal conductance. *Plant, Cell and Environment* **26**, 1767–1785.

Buckley T.N., Sack L. & Gilbert M.E. (2011) The role of bundle sheath extensions and life form in stomatal responses to leaf water status. *Plant Physiology* **156**, 962–973.

Comstock J. & Mencuccini M. (1998) Control of stomatal conductance by leaf water potential in Hymenoclea salsola (T & G), a desert subshrub. *Plant, Cell and Environment* **21**, 1029–1038.

Farquhar G.D., von Caemmerer S. & Berry J.A. (1980) A biochemical model of photosynthetic CO2 assimilation in leaves of C3 species. *Planta* **149**, 78–90.

Farquhar G.D. & Wong S.C. (1984) An empirical model of stomatal conductance. *Australian Journal of Plant Physiology* **11**, 191–210.

Gates D.M., Keegan H.J., Schleter J.C. & Weidner V.R. (1965) Spectral properties of plants. *Applied optics* **4**, 11–20.

Leuning R. (1995) A critical appraisal of a combined stomatal-photosynthesis model for C3 plants. *Plant, Cell & Environment* **18**, 339–355.

McAdam S.A. & Brodribb T.J. (2016) Linking turgor with ABA biosynthesis: implications for stomatal responses to vapour pressure deficit across land plants. *Plant Physiology* **171**, 2008–2016.

Medlyn B.E., Duursma R.A., Eamus D., Ellsworth D.S., Prentice I.C., Barton C.V.M., … Wingate L. (2011) Reconciling the optimal and empirical approaches to modelling stomatal conductance. *Global Change Biology* **17**, 2134–2144.

Mott K.A. (2007) Leaf hydraulic conductivity and stomatal responses to humidity in amphistomatous leaves. *Plant, Cell and Environment* **30**, 1444–1449.

Mott K.A., Denne F. & Powell J. (1997) Interactions among stomatal in response to perturbations in humidity. *Plant, Cell and Environment* **20**, 1098–1107.

Mott K.A. & Parkhurst D.F. (1991) Stomatal responses to humidity in air and helox. *Plant, Cell and Environment* **14**, 509–515.

Oren R., Sperry J.S., Katul G.G., Pataki D.E., Ewers B.E., Phillips N. & Schafer K.V.R. (1999) Survey and synthesis of intra- and interspecific variation in stomatal sensitivity to vapour pressure deficit. *Plant, Cell and Environment* **22**, 1515–1526.

Peak D. & Mott K.A. (2011) A new, vapour-phase mechanism for stomatal responses to humidity and temperature. *Plant, Cell & Environment* **34**, 162–178.

Prentice I.C., Dong N., Gleason S.M., Maire V. & Wright I.J. (2014) Balancing the costs of carbon gain and water transport: testing a new theoretical framework for plant functional ecology. *Ecology letters* **17**, 82–91.

de Pury D.G.G. & Farquhar G.D. (1997) Simple scaling of photosynthesis from leaves to canopies without the errors of big-leaf models. *Plant, Cell and Environment* **20**, 537–557.

Rockwell F.E., Holbrook N.M. & Stroock A.D. (2014) The competition between liquid and vapor transport in transpiring leaves. *Plant Physiology* **164**, 1741–1758.

Saliendra N.Z., Sperry J.S. & Comstock J.P. (1995) Influence of leaf water status on stomatal response to humidity, hydraulic conductance, and soil drought in Betula occidentalis. *Planta* **196**, 357–366.

Shackel K.A. & Brinkmann E. (1985) In situ measurement of epidermal cell turgor, leaf water potential, and gas exchange in Tradescantia virginiana L. *Plant Physiology* **78**, 66–70.

Sussmilch F.C., Brodribb T.J. & McAdam S.A. (2017) Up-regulation of NCED3 and ABA biosynthesis occur within minutes of a decrease in leaf turgor but AHK1 is not required. *Journal of Experimental Botany* **68**, 2913–2918.

Xie X., Wang Y., Williamson L., Holroyd G.H., Tagliavia C., Murchie E., … Hetherington A.M. (2006) The identification of genes involved in the stomatal response to reduced atmospheric relative humidity. *Current Biology* **16**, 882–887.